Whirl Flutter Test of Swept-Tip Tiltrotor Blades



James Sutherland*
Clark Doctoral Fellow

Frederick Tsai
Graduate Research Assistant
University of Maryland, College Park, MD

Anubhav Datta
Associate Professor

The first whirl flutter test of the Maryland Tiltrotor Rig (MTR) was recently completed in the Naval Surface Warfare Center Carderock Division (NSWCCD) 8- by 10-ft large subsonic wind tunnel. The MTR is a Froude-scaled, 4.75 ft diameter, three-bladed, semispan, floor-mounted, optionally powered, flutter rig. This paper focuses on the swept-tip blades developed for this test. The swept-tip begins at 80%R and sweeps aft 20° to alleviate whirl flutter. Whirl flutter testing was performed in four configurations for both blade geometries. The frequency and damping of the wing beam and chord bending were collected at wind speeds up to 100 kt. This paper directly compares whirl flutter results between the straight and swept-tip blades and demonstrates higher wing chord damping using swept-tip blades in freewheel conditions, even at lower flight speeds.

Nomenclature

C_T	rotor thrust coefficient
c.g.	center of gravity
M_{tip}	tip Mach number
$\%R$	percentage of rotor radius
r	spanwise location along the blade, m
γ_{xy}	shear strain
ϵ_i	strain in the i direction
θ_{75}	collective pitch angle at 75% radius
σ	rotor solidity ratio

Introduction

Dramatic expansions of speed, range, and payload are desired for future vertical lift aircraft. Tiltrotor aircraft combine the vertical takeoff and landing ability of a helicopter with the cruise ability of fixed-wing aircraft to perform many long-range and high-speed missions. A grand vision for the future is to achieve speeds up to 350–400 kt in cruise as seen in modern turboprop aircraft. Significant amounts of research, time, and energy are required to achieve these goals. The Maryland Tiltrotor Rig (MTR) provides the test bed to invest those resources and achieve the goals of high-speed tiltrotor flight. The conceptual design of the rig was described in Ref. 2, and the construction of the gimballed hub model in Ref. 3. The structural design, modeling, and testing of the rotor blades were described in Refs. 4 and 5.

The first whirl flutter test of the MTR was recently completed in the Naval Surface Warfare Center Carderock Division (NSWCCD) 8- by 10-ft large subsonic wind tunnel (SWT). Two sets of whirl flutter data were acquired: one for straight blades (baseline) and another for swept-tip blades. This paper is focused on the data acquired with the swept-tip blades. An overview of the test was presented in Ref. 6. Correlation of test and analysis was presented in Ref. 7.

It is well known that the fundamental barrier to high flight speed in tiltrotors is whirl flutter. Whirl flutter is a destructive, aeroelastic instability between the flapping rotor and the wing that limits the cruise speed in airplane mode. Whirl flutter is solved today by stiffening the wing, which historically requires increasing the wing thickness and the drag of the aircraft, thereby increasing power requirements and reducing mission performance. In order to push the boundaries of tiltrotor flight, advanced hub, and rotor geometries must be studied that will allow for thinner wings that are also flutter free.

Numerous model-scale tests have been performed to gain a more fundamental understanding of tiltrotor whirl flutter. In 1975, the Boeing Vertol Company built two 2.8-ft Froude-scale models, and these were tested in the Wright Brothers wind tunnel at MIT (Refs. 8, 9). The models measured gust stability. As part of the V-22 development, Bell conducted a series of systematic tests on a 1/5th scale model (Ref. 10). These tests lead to the evolution of the XV-15 hub and ultimately the V-22 hub. The right-hand wing and rotor of this model later became the Wing and Rotor Aeroelastic Test System (WRATS) (Refs. 11, 12). The WRATS test rig was used to study a number of parametric variations to study their effect on tiltrotor whirl flutter. However, the parametric variations were limited to control system stiffness, pitch–flap coupling, and test medium. A contemporary effort is the TiltRotor Aeroelastic Stability Testbed (TRAST) developed by the U.S. Army, but whirl flutter test data have not yet been published (Ref. 13). Two other important tiltrotor scaled models are the Sikorsky's Variable Diameter Tilt Rotor (VDTR) (Ref. 14) and NASA's Tiltrotor Aeroacoustic Models (TRAM) (Ref. 15). But, neither of these models was tested for whirl flutter.

*Corresponding author; email: james.r.sutherland2@boeing.com.
Paper previously presented at AIAA SciTech, San Diego, CA, January 3–7, 2022 (Ref. 1). Manuscript received February 2022; accepted April 2023.

DOI: 10.4050/JAHS.69.012010

(a) Straight, unwisted blade

(b) Straight, twisted blade (baseline)

(c) Swept-tip blade

Fig. 1. The family of blade geometries designed and built for testing on the MTR.

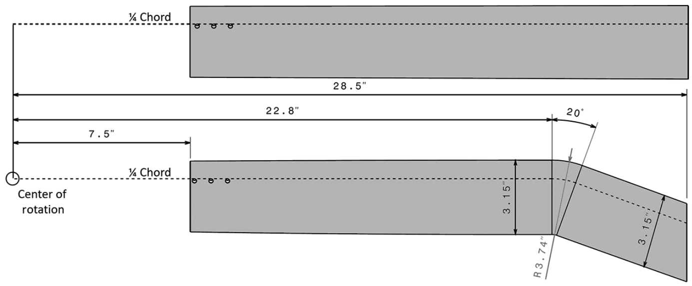

Fig. 2. Planform dimensions of the straight and swept-tip blades. Dimensions in inches.

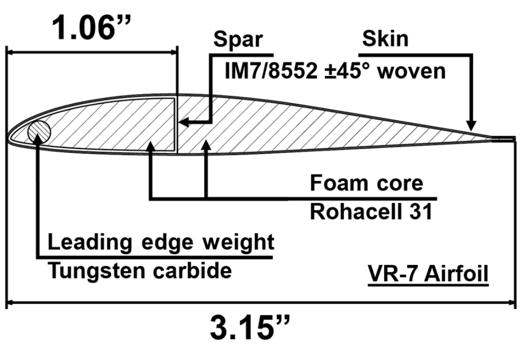

(a) Sketch of uniform cross section

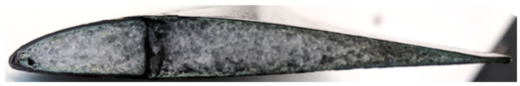

(b) Cross section of a fabricated blade section

Fig. 3. Designed and fabricated cross section of the parametric blade family.

Unfortunately, many of these tests utilized models with proprietary information that is not publicly available. On the whole, previous and current tiltrotor aeroelastic tests have focused on a single rotor geometry: straight proprotor blades on a gimballed hub. Thus, there is a lack of high-quality, publicly available, parametric test data and properties on whirl flutter. The MTR was designed to address this need for new parametric test data.

Previous comprehensive analyses on blade geometry and composite coupling (Refs. 16–19) have shown that pitch–flap and pitch–lag coupling due to a large sweep angle is likely to stabilize whirl flutter by increasing the damping of the wing bending modes. However, there has been no experimental verification of this conclusion nor a clear understanding of the physics. The Advanced Technology Blades for XV-15 did include a swept tip but was only tested in hover (Ref. 20). The ONERA Adyn Blade design was tested in whirl flutter, but there is no parametric data available and the tip utilized a double sweep designed for acoustics, not dynamics (Refs. 21, 22). This work is one of the first efforts testing swept-tip blades to understand their impact on tiltrotor whirl flutter. A previous paper reported on the pretest predictions of blade stresses and strains to ensure a safe wind tunnel test (Ref. 4). This paper now reports the test data.

This paper begins with a description of the blade design before discussing integration of the swept-tip blades into the MTR. Next, a brief overview of the first whirl flutter tests performed at the NSWCCD SWT is provided. Finally, the frequency and damping of the wing bending modes at wind speeds up to 100 kt are discussed for all eight test configurations, with specific comparison of the straight blades and swept-tip blade geometries.

Blade Design

The MTR was designed for testing in the Glenn L. Martin Wind Tunnel. Based on the size of the test section, 7.75- by 11-ft, the maximum rotor diameter was fixed at 4.75 ft. With a uniform chord length of 3.15 inches and a root cutout of 27%R, the three-bladed rotor has a solidity of 0.078.

There are three distinct blade geometries that make up the family of blades developed in this work. The blades are shown in Fig. 1. Each blade is comprised of a uniform VR-7 airfoil cross section. The first blade is straight and untwisted and is used for structural property measurement. The second blade, also referred to as the baseline or "straight blade," has a straight quarter chord and is twisted -37° over the span. High twist is necessary for tiltrotor blades due to the high inflow experienced during cruise. The final blade, referred to as the "swept-tip blade", is also twisted but adds a tip sweep of 20° starting at 80%R. The airfoil section and geometric twist for the swept tip are defined in reference to the swept quarter-chord line. The planform for the straight and swept-tip blades is shown in Fig. 2. Figures 3(a) and 3(b) show the designed and fabricated cross section used across each blade.

The swept-tip blade planform has three distinct sections. First, the straight section, which is identical to the straight, twisted blade and extends to 80%R. Next, there is a rounded transition region. It follows a circular arc of 20° because a sharp corner cannot be fabricated accurately and can lead to local ply separation. Finally, the swept region extends from the end of the transition region to the blade tip. In the swept region, the linear twist rate is defined with respect to the local quarter-chord line. Additionally, the twist in the transition region must be reduced to lessen the curvature between the straight and swept portions at the trailing edge. The designed twist distribution is listed in Table 1 and shown in Fig. 4 with markers indicating the locations of prescribed twist angles.

While the MTR and rotor blades are not designed to match any specific aircraft, the 1/5.26 Froude scale XV-15 blade properties are used as loose targets. To achieve this, a 2-ply spar ending at

Table 1. Twist distribution

	r/R	θ (deg) Straight	θ (deg) Swept-Tip
	0	–	–
Blade root	0.263	18	18
Sweep start	0.800	−1.85	−1.85
Transition end	0.835	−3.15	−2.10
Blade tip	1.000	−9.25	−8.59

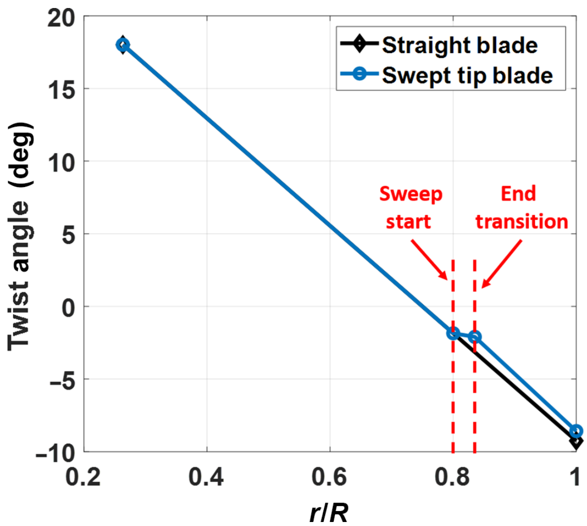

Fig. 4. Twist of the straight and swept-tip blades about the local 1/4 chord.

33% chord was selected to match the target normal stiffness while achieving the lowest chord stiffness possible. The cross-sectional center of gravity (c.g.) is placed near 25% chord using leading edge weights. The cross-section design and fabrication materials are shown in Fig. 3(a).

The cross section of the swept-tip is comprised of only the foam core and blade skin. Based on the findings of Ref. 19, the effect of the swept-tip is primarily due to the aerodynamic offset, not the c.g., so the spar and leading edge weights do not extend into the swept or transition portions of the blade. Extending the leading edge weights into the swept region would shift the overall c.g. of the blade further aft and cause an inertial coupling that would oppose the aerodynamic coupling introduced by the swept-tip and reduce its potential effectiveness. The spar is not necessary in the swept region and is avoided to prevent adding to the complexity of the structure and concerns of c.g. placement for pitch–flap flutter.

The straight, untwisted blades' sectional properties were characterized. The baseline and swept-tip blades were then tested in a vacuum chamber to measure rotating frequencies and strains. Three-dimensional (3D) finite element based models were developed, validated with vacuum chamber data, and numerically stress-tested with free-wake-based comprehensive analysis. These details have been documented in Ref. 4. The sectional blade properties are described in Table 2. More general properties for the MTR as a whole are outlined in Ref. 23. The properties of the straight section were measured and used to validate the structural model of the 3D finite element analysis. The properties of the swept section are with respect to the local quarter-chord line; they were not measured but predicted based on the finite element model. Based on these predictions,

Table 2. Cross-sectional properties of the blade sections; straight section is measured; swept section is predicted by X3D.

	Straight Section		Swept Section	
Radial Station, r/R	0.27	0.8	0.835	1.0
$\frac{1}{4}$ chord location				
y (cm)	0	0	−0.447	−4.79
z (cm)	0	0	0	0
Chord (cm)	8.0	8.0	8.0	8.0
Mass/length (kg/m)	0.33	0.33	0.15	0.15
Center of gravity (% c)	27%	27%	45%	45%
EI_N (Nm^2)	20.1	20.1	12.0	12.0
EI_C (Nm^2)	937	937	534	534
GJ (Nm^2)	62	62	36.8	36.8

removing the leading edge weights reduces the sectional mass by 55% while removing the spar reduces the sectional stiffness 40–45% in each direction. The fabricated swept-tip blade has a mass of 151 g, 25 g lighter than the baseline blade. The net result is the swept-tip blade has slightly higher natural frequencies than the baseline blade.

Maryland Tiltrotor Rig Integration

In addition to many other features, the MTR was designed to allow for interchangeable blades. With the straight blades already installed, the process of changing to the swept-tip blade only required a few minutes. The pitch case and blade grip adapter are common between blade sets, so only three bolts and sensor connections need to be changed. First, the nose cone was removed to allow access to the hub components and instrumentation plate. Next, all blade strain gauge wires were disconnected from the instrumentation plate at the hub. Then the three 9/16″ shoulder bolts connecting the straight blade to the grip adapter were unfastened, allowing for the removal of the blade. The swept-tip blade was installed with the same bolts. Although all three blades have normal and chord bending moment gauges, only four channels are available to record strain data. Therefore, the normal and chord strain bridges from two blades were installed. The excess length, as well as unconnected wires, were carefully wrapped around the pitch case and secured with metallic tape to ensure enough slack for full collective motion of the hub. Last, the strain gauge connections were verified with rap tests and static deflections of the blade.

Prior to installation, metallic tape was placed at the end of the straight section to ensure proper balance. The blades were balanced in pairs to ensure similar spanwise c.g. position. Additionally, retroreflective tape was adhered to the blade tip cross section to allow for blade tracking. A light strobing at 3/rev was aimed at the edge of the rotor disc, illuminating each blade as it passed. This was first done with the rotor spinning at 300 RPM and progressing to the nominal speed of 1050 RPM. With the swashplate level, the flap deflection discrepancy between each blade was less than one airfoil thickness and there was no discernible difference in lag deflection. No adjustments were needed, but the pitch links of each blade are adjustable in length to ensure uniform tracking in flap.

Whirl Flutter Test Procedure

The MTR was installed in the SWT located at the NSWCCD as shown in Fig. 5. Although the MTR was designed for the Glenn. L. Martin Wind Tunnel, the SWT has a similar cross section, 8- by 10-ft, and maximum speed of 163 kt. The approved test envelope, however, only extended up to 100 kt. The full test overview is described in greater detail in Ref. 6.

Table 3. Flutter test conditions

Sweep	Tunnel Speed (kt)	Collective (deg)	Gimbal	Mode	Wing Assembly
Straight blades					
Set 2					
1	30, 40, 50, 60, 65, 70, 74, 78, 82, 86, 89, 92, 96, 100	9.9, 17.6, 22.3, 26.7, 28.2, 30.0, 31.2, 32.8, 34.1, 35.4, 36.8, 37.5, 38.8, 39.8	Free	Freewheel	On
2	30, 40, 50, 60, 65, 70, 74, 78, 82, 86, 89, 92, 96, 100	10.4, 17.3, 22.4, 26.5, 28.6, 30.5, 31.7, 33.4, 34.6, 35.9, 36.8, 37.9, 39.1, 40.1	Free	Freewheel	Off
Set 1					
3	30, 40, 50, 60	11.3, 17.2, 22.1, 26.4	Locked	Freewheel	Off
4	4, 20, 30, 40, 50, 60	3.2, 11.4, 15.8, 20.7, 25.2, 28.9	Locked	Powered	Off
Swept-tip blades					
5	30, 40, 50, 60, 65, 70, 74, 78, 82, 86, 89, 92, 96, 100	13.3, 18.9, 23.5, 27.4, 29.5, 31.2, 32.4, 34.3, 35.2, 37.1, 37.9, 39.0, 39.9, 40.7	Free	Freewheel	On
6	30, 40, 50, 60, 65, 70, 74, 78, 82, 86, 89, 92, 96, 100	11.9, 17.8, 22.0, 26.4, 28.8, 30.8, 32.5, 33.8, 35.1, 36.3, 37.8, 38.7, 39.6, 40.6	Free	Freewheel	Off
7	30, 40, 50, 60, 65, 70, 74, 78, 82	11.1, 17.1, 22.1, 26.5, 29.1, 31.4, 32.7, 34.3, 35.1	Locked	Freewheel	Off
8	4, 20, 30, 40, 50, 60	3.4, 13.0, 16.9, 21.6, 25.9, 29.7	Locked	Powered	Off

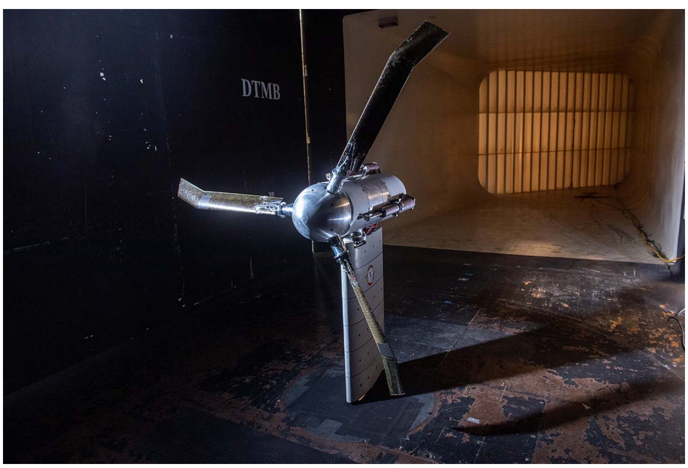

Fig. 5. The swept-tip blades installed on the MTR in the SWT.

Fig. 6. The MTR installed with wing fairings removed and baseline blades installed.

Flutter test points were collected at nominal wind speeds for the wing beam and wing chord modes. At least three trials were performed per wing mode. The test conditions are shown in Table 3. Whirl flutter tests were performed with four major parametric changes, each performing a sweep of wind speed. The baseline configuration, Sweep 1, is the gimballed rotor with the twisted blades installed; the rotor is unpowered in a freewheel condition. In Sweep 2, the wing fairing was removed to study the effect of wing aerodynamics on flutter stability. Figure 6 shows the MTR supported by the spar with wing fairing removed. With the wing fairings off, the gimbal was locked in Sweep 3, resulting in a stiff-inplane hingeless rotor. Finally, in Sweep 4, the rotor was powered by the electric motor to compare with results in the freewheel mode. The configuration in Sweeps 5–8 is identical to the first 4 with the exception of having the swept-tip blades installed.

To conduct the flutter test in freewheel conditions, the tunnel was set to the desired wind speed while the collective was adjusted to maintain 1050 RPM. When the gimbal was not locked, the rotor was trimmed using cyclic controls. Under powered conditions, the motor throttle controlled RPM and the rotor was trimmed to a constant thrust using collective pitch. Once at the specified condition, the swashplate was perturbed in order to excite the wing bending modes. For beam bending excitation, an approximately 0.5° perturbation in longitudinal cyclic at

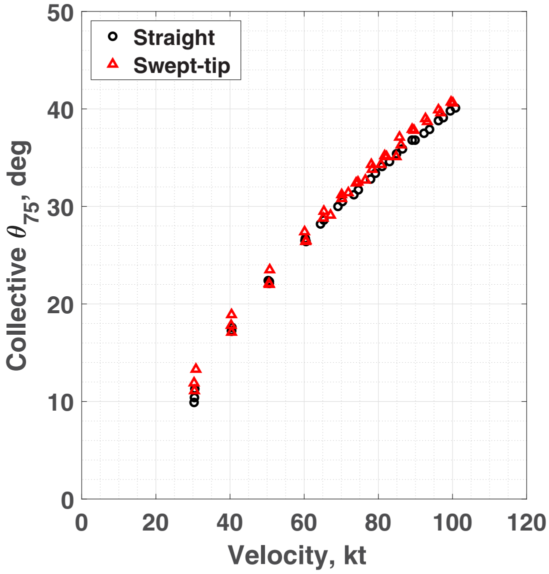

Fig. 7. Collective, θ_{75}, required to maintain 1050 RPM at each wind speed for straight and swept-tip blades.

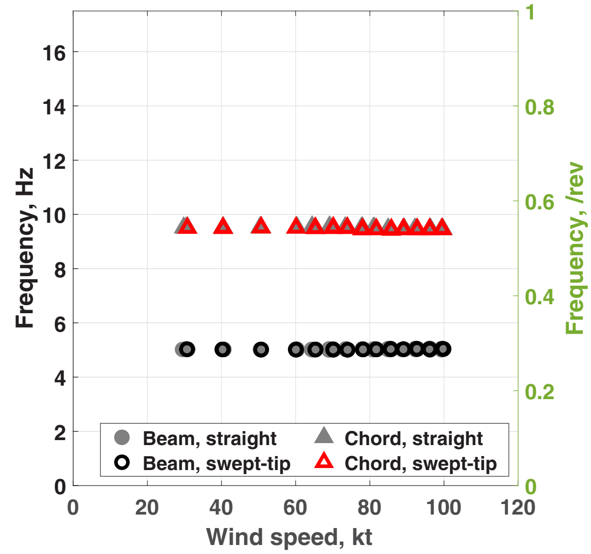

Fig. 8. Measured frequency of the wing beam and chord bending in the wing on, gimbal free, freewheel configuration (Sweeps 1 and 5).

the wing beam frequency was applied while recording the strain at the root of the wing spar. For chord bending excitation, a 0.5° perturbation in collective at the wing chord frequency was applied. Three trials were performed for each bending mode at each wind speed; Ref. 23 describes the moving block method which was used to extract the signal damping.

Whirl Flutter Results

The results of the baseline twisted blades are presented and discussed in detail in Ref. 6. Because each configuration was tested with both blade sets, this paper draws direct comparisons between the straight and swept-tip blades in each configuration. Figure 7 shows the collective setting of each blade, θ_{75}, required for the MTR to maintain 1050 RPM at each speed. The correlation between the blades indicates the swept-tip blades are aerodynamically similar to the straight blades.

For all Figures 8–12(b), the symbols show the measured frequency or damping during each individual trial. Squares symbolize values of wing chord frequency and damping, while triangles symbolize the wing beam mode. Results for the straight blade are plotted in gray, while the swept-tip blade results are plotted in red for chord and black for beam bending modes. All frequency and damping measurements are printed in Tables 5–12 in the Appendix.

The wing structural damping was measured to be 0.4% in the beam mode and 0.57% in the chord mode. Since this was the first whirl flutter test entry for the MTR, and the first stability test in the SWT, initial testing proceeded cautiously, but at these low damping values the MTR showed very little response to any natural perturbations in airflow. After swashplate perturbation, a safety officer was able to visibly watch the wing vibrations damp out while the test engineer observed the wing strain decay at the same rate. Observing the test rig's stability and response to perturbation provided the confidence necessary to proceed to higher wind speeds.

Baseline configurations

In Sweeps 1 and 5, the baseline configuration, the gimballed rotor was in a freewheeling condition and the wing fairings were installed. As summarized in Table 4, Fig. 8 shows no change to the wing bending frequencies in the baseline configuration; the same conclusion can be made for the each subsequent configuration and so those results are omitted. Figures 9(a) and 9(b) show the measured damping of the wing beam and chord bending modes in the baseline configuration.

Table 4. Measured frequencies of wing beam and chord modes in each configuration with both blade sets

	Beam Frequency (Hz)		Chord Frequency (Hz)	
	Straight	Swept-Tip	Straight	Swept-Tip
Sweeps 1, 4	5.04	5.06	9.45	9.39
Sweeps 2, 5	5.05	5.06	9.47	9.39
Sweeps 3, 6	5.05	5.03	9.45	9.44
Sweeps 7, 8	5.03	5.03	9.49	9.48

For both blade sets, the damping of the beam mode starts low, approximately 0.5% critical, and gradually grows to approximately 1% critical. At low speeds, there is no noticeable difference between the beam damping of the straight and swept-tip blades. At higher speeds, there is larger scatter between each trial. However, the beam damping with the swept-tip blades installed appears to increase more than when the straight blades are installed. Looking at the chord mode, the damping gradually decreases from approximately 1.5–1.2% critical. At wind speeds greater than 86 kt, there is an apparent (less than 10%) increase in the wing chord damping ratio when the swept-tip blades are installed. These results appear to be consistent with trends presented in Refs. 16 and 19, where blade tip sweep has a more pronounced effect on the wing chord damping than the beam damping. However, both previous numerical studies predict a much larger increase in wing damping when the blade tip is swept 20° aft.

Wing-off configurations

In Sweeps 2 and 6, the MTR had the gimballed rotor in a freewheeling condition and the wing fairings were removed. Thus, the only effect

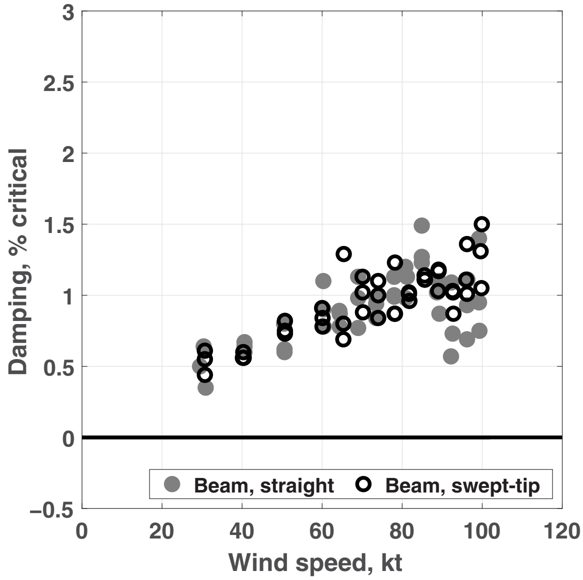

(a) Measured damping of the wing beam bending

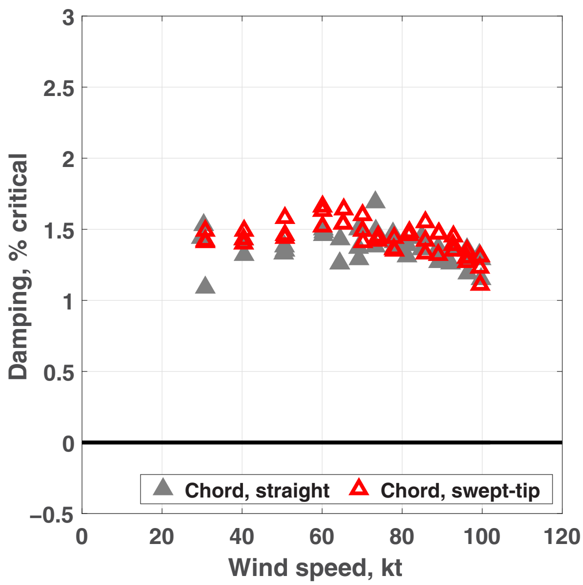

(b) Measured damping of the wing chord bending

Fig. 9. Wing beam and chord damping in the wing on, gimbal free, freewheel configuration (Sweeps 1 and 5).

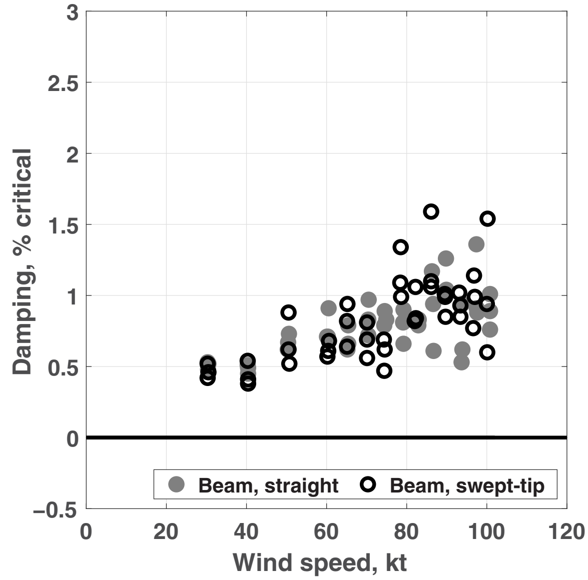

(a) Measured damping of the wing beam bending

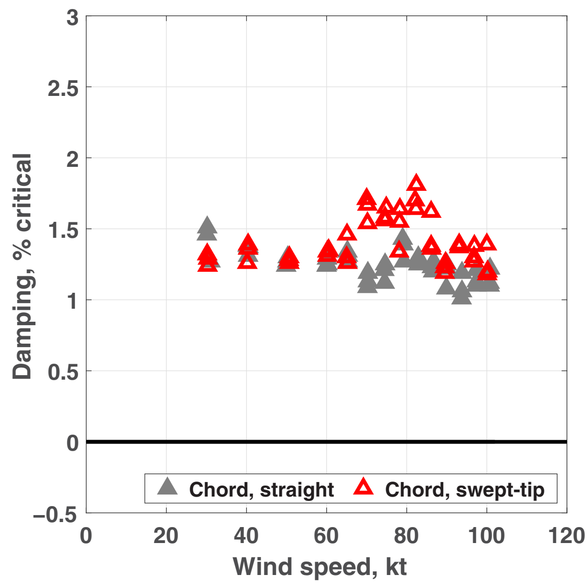

(b) Measured damping of the wing chord bending

Fig. 10. Wing beam and chord damping in the wing off, gimbal free, freewheel configuration (Sweeps 2 and 6).

on the results, when compared to Sweeps 1 and 5, should be due to aerodynamics of the wing. In Figs. 10(a) and 10(b), the same general trends of the baseline configuration are observed. The beam damping increases from approximately 0.5% critical and gradually grows to approximately 1% critical. The chord mode decreases at a lower rate than with the wing installed from 1.3% critical on average to 1.2% critical over the 100-kt sweep.

The swept-tip beam mode damping follows closely with the straight blade results with variations within the data scatter. The damping of the wing chord mode is relatively unaffected by blade geometry up to 60 kt. Between 70 and 86 kt, the swept-tip blade shows a 45% increase in wing chord damping ratio, from 1.1% critical to 1.6% critical over the straight blades before returning back to the same apparent increase observed with the wing fairings installed. This jump indicates that even though the effects of sweep are expected to take effect at higher speeds, there are measurable differences at lower speeds. However, the cause is unknown and presents an interesting case for further analysis and predictions to understand.

Gimbal-locked configurations

In Sweeps 3 and 7, the rotor gimbal was locked but still freewheeling and the wing fairings are removed. The gimbal-locked condition approximates a stiff in-plane hingeless hub with a first flap frequency of 1.8/rev. Since flight with the gimbal locked was predicted to have higher damping (Ref. 7), testing in this condition was performed prior to the gimballed rotor testing. In order to build confidence in the test rig, initial sweeps only reached 60 kt until enough data was collected to safely proceed to

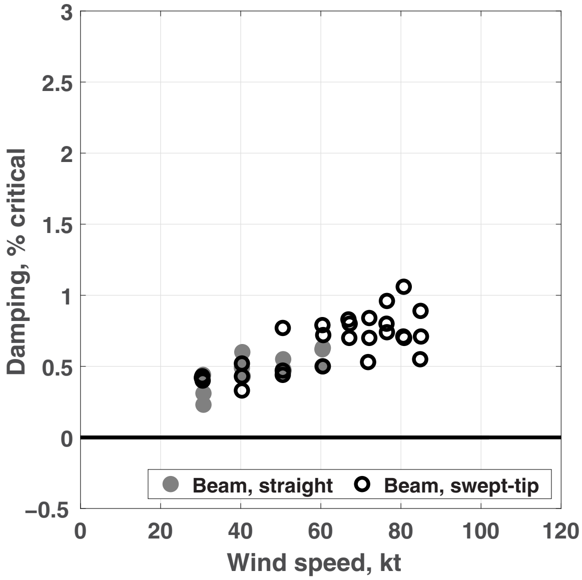

(a) Measured damping of the wing beam bending

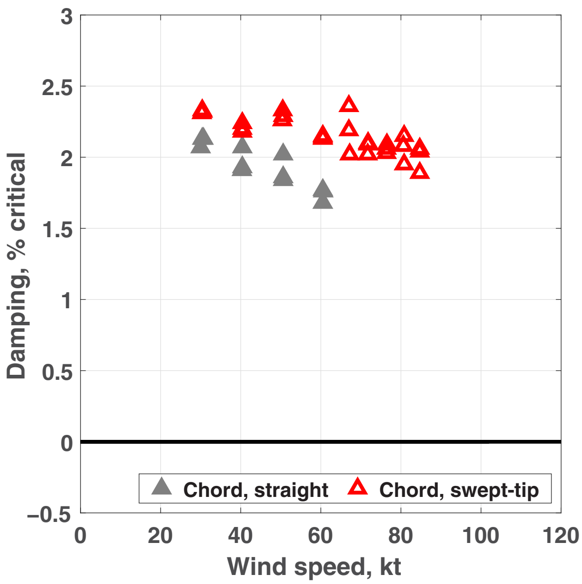

(b) Measured damping of the wing chord bending

Fig. 11. Wing beam and chord damping in the wing off, gimbal locked, freewheel configuration (Sweeps 3 and 7).

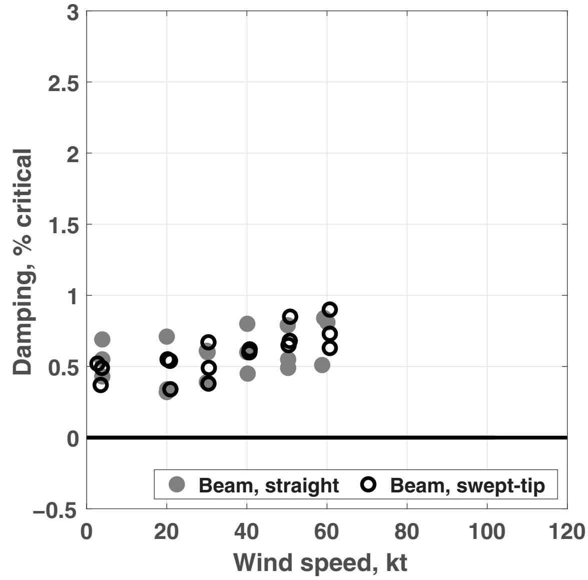

(a) Measured damping of the wing beam bending

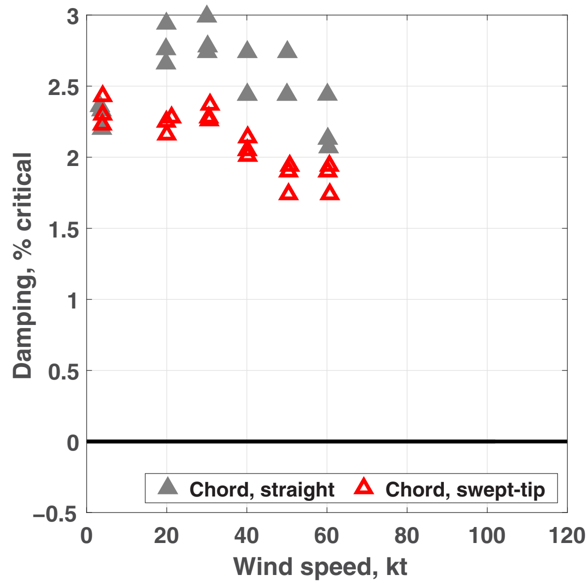

(b) Measured damping of the wing chord bending

Fig. 12. Wing beam and chord damping in the wing off, gimbal locked, powered configuration (Sweeps 4 and 8).

82 kt and ultimately 100 kt. Unfortunately, due to limited test time, earlier runs were not able to be revisited and tested to the full range of speeds. Although the wind speed of Sweep 3 only covers 20–60 kt, Sweep 7 goes up to 82 kt.

Figures 11(a) and 11(b) show the measured beam and chord damping of the wing for each test point. The wing beam damping shows the same overall trend as the gimbal free case, but the wing chord damping is over 2% critical, an 80% increase from the gimbal-free case. When comparing the blade sets, no noticeable difference in wing beam damping can be observed between the straight and swept-tip blades. However, the swept-tip blades have a strong effect on chord damping. At 30 kt, the swept-tip blade increases the wing chord damping by 10% from 2.1% critical to 2.3% critical. As wind speed increases, the wing chord damping decreases linearly for both sweeps, but the measured damping of Sweep 7 decreases at less than half the rate of Sweep 3. Based on these results, locking the gimbal drastically increases the wing chord damping compared to the gimballed rotor and the swept-tip blade further adds to the benefit. The Sweep 7 test conditions provide the largest benefit to wing chord damping out of all freewheel configurations.

Powered configurations

In Sweeps 4 and 8, the rotor gimbal was locked, the motor was powered on, and the wing fairings were removed. Due to electromagnetic interference between the motor and load cell, thrust measurements were not reliable, so the collective was set based on predictions from Ref. 7 for zero thrust. Although the first test point was tested with the tunnel power off, the rotor recirculates flow through the wind tunnel and induces a 4-kt wind in the test section. Looking at the wing damping, Figs. 12(a) and

12(b) show minimal difference in the wing beam bending between the straight and swept-tip blade sets.

Comparing Sweeps 4 and 8 to Sweeps 3 and 7 demonstrates the effect of powering the rotor versus freewheeling. When the rotor is powered, the wing beam damping ratio increases by approximately 15% across all tested wind speeds. The straight and swept-tip blades have very similar results for the wing beam damping ratio. When the rotor is powered, the wing chord damping also sees a dramatic increase, as has been observed historically. However, the swept-tip causes a 20% decrease in the measured chord damping, from 2.54% critical to 2.06% critical at 50 kt. The opposite effect is observed in all freewheeling cases. While the test data show the effect of swept-tip, there is not yet an obvious answer to why it causes such a dramatic decrease in the chord damping while in the powered configuration. Therefore, it is critical to investigate how the combination of different parameter changes affects the wing damping in combination, not only in isolation.

Conclusions

In summary, this work presents the measured wing frequencies and damping of a Froude-scale model tiltrotor with straight and swept-tip blades. A large swept-tip was added to the baseline twisted blade to introduce aerodynamic coupling and potentially delay whirl flutter. The blades were installed on the MTR, and whirl flutter tests were carried out in the SWT located at the NSWCCD. The whirl flutter tests followed systematic variation of parameters including comparisons of wing aerodynamics, gimballed versus hingeless, freewheel versus powered flight, and straight versus swept-tip blades. Thus, there are enough significant differences introduced by the swept-tip, even at lower speeds, to provide a rich dataset of validation data for advanced analysis. Based on these results, the following conclusions are drawn:

1) The MTR was successfully tested with measured wing damping ratios of 0.5% up to 100 kt.

2) The wing beam mode damping shows little change between the straight and swept-tip blades up to 100 kt.

3) In the gimbal-locked configuration, the swept-tip blades provide a strong benefit to wing chord damping. At 30 kt, the damping ratio is 10% higher than the baseline blade and the downward sloping trend is reduced by a factor of 2.

4) The scatter in the data prevents broad conclusions about the effect of swept-tip blades in the baseline (Sweeps 1,5) and wing-off (Sweeps 2,6) configurations. However, with the swept-tip blades installed, a small increase in damping can be observed in the beam and chord modes above 83 kt wind speed, which indicates a potential benefit and presents an interesting case for further analysis and predictions to understand.

5) Compared to the gimballed hub results, locking the gimbal (stiff-inplane hingeless hub) results in an 80% increase in the wing chord mode damping ratio.

6) Powered flight conditions are more highly damped than freewheel flight; however, the swept-tip blade causes a 20% reduction in wing chord damping.

7) The wing bending frequencies are changed by less than 1% when changing blade geometry.

Future work consists of expanding the range of speeds where the aerodynamic coupling introduced by the swept-tip is stronger as well as hover tests to compare rotor performance, loads, and vibration.

Acknowledgments

This work is carried out at the Alfred Gessow Rotorcraft Center, University of Maryland at College Park under the Army/Navy/NASA Vertical Lift Research Center of Excellence (VLRCOE) grant number W911W61120012 with technical monitoring from Mahendra Bhagwat and points of contact Tom Parham (Bell), Hyeonsoo Yeo (Army), C.W. Acree, Jr (NASA), and Wayne Johnson (NASA). Additional funding for blade fabrication and instrumentation hardware was provided by Naval Air Warfare Center Aircraft Division seed grant with technical monitoring from Ronald Barry Walden (2018–2019) and Mark Silva (2019–2020). The carbon fiber material used to fabricate the blade was donated by the Boeing Company.

Appendix

Table 5. Measured damping of wing beam mode during Sweeps 1 and 5, the baseline configuration

Straight Blades			Swept-Tip Blades		
Wind Speed (kt)	Frequency (Hz)	Damping (% critical)	Wind Speed (kt)	Frequency (Hz)	Damping (% critical)
29.5	5.02	0.50	30.7	5.03	0.44
30.4	5.04	0.64	30.7	5.02	0.55
30.9	5.03	0.35	30.7	5.03	0.61
40.6	5.02	0.60	40.4	5.02	0.56
40.6	5.02	0.64	40.2	5.02	0.56
40.6	5.02	0.67	40.3	5.02	0.60
50.6	5.01	0.62	50.7	5.02	0.82
50.5	5.02	0.80	50.7	5.02	0.73
50.6	5.01	0.60	50.7	5.01	0.75
60.3	5.03	1.10	60.0	5.02	0.91
60.3	5.03	0.90	60.1	5.01	0.78
60.4	5.02	0.78	60.1	5.01	0.84
64.4	5.02	0.78	65.3	5.01	0.80
64.3	5.02	0.89	65.3	5.02	0.69
64.4	5.01	0.87	65.4	5.02	1.29
69.0	5.00	0.98	70.1	5.01	1.13
69.0	5.04	0.77	70.1	5.03	1.02
69.0	5.02	1.13	70.2	5.01	0.88
73.5	5.04	0.94	74.0	5.01	1.00
73.6	5.03	0.98	74.0	5.01	1.10
73.5	5.02	0.84	74.0	5.01	0.84
78.0	5.04	0.99	78.1	5.02	0.87
78.0	5.03	1.00	78.2	5.02	1.23
78.0	5.04	1.13	78.2	5.02	0.87
80.8	5.01	1.20	81.8	5.02	0.96
80.9	5.03	0.98	81.7	5.02	1.02
81.2	5.04	1.13	81.7	5.03	1.01
84.9	5.02	1.27	85.6	5.03	1.14
84.9	5.02	1.23	85.7	5.02	1.11
84.9	5.05	1.49	85.6	5.05	1.11
89.3	5.02	0.87	89.0	5.03	1.03
88.7	5.02	1.02	89.1	5.03	1.17
89.1	5.03	1.10	89.1	5.03	1.18
92.6	5.03	0.73	92.8	5.04	0.87
92.3	5.02	1.09	92.7	5.03	1.02
92.2	5.05	0.57	92.6	5.05	1.03
96.2	5.06	0.69	96.0	5.04	1.11
96.3	5.03	1.11	96.2	5.01	1.01
96.2	5.02	0.93	96.2	5.03	1.36
99.3	5.01	0.75	99.6	5.05	1.31
99.2	5.04	0.95	99.8	5.03	1.05
99.2	5.04	1.40	99.9	5.04	1.50

Table 6. Measured damping of wing chord mode during Sweeps 1 and 5, the baseline configuration

Straight Blades			Swept-Tip Blades		
Wind Speed (kt)	Frequency (Hz)	Damping (% critical)	Wind Speed (kt)	Frequency (Hz)	Damping (% critical)
30.8	9.52	1.09	30.8	9.50	1.49
30.4	9.50	1.53	30.8	9.50	1.41
29.8	9.51	1.44	30.8	9.50	1.42
40.4	9.50	1.43	40.4	9.50	1.43
40.4	9.52	1.40	40.5	9.49	1.49
40.5	9.51	1.32	40.4	9.51	1.40
50.4	9.52	1.33	50.7	9.52	1.44
50.7	9.51	1.35	50.7	9.51	1.58
50.6	9.51	1.38	50.7	9.52	1.46
60.3	9.51	1.46	60.1	9.51	1.52
60.4	9.51	1.48	60.1	9.51	1.66
60.3	9.51	1.50	60.1	9.51	1.63
64.4	9.53	1.26	65.2	9.49	1.54
64.5	9.54	1.43	65.3	9.50	1.54
64.4	9.54	1.26	65.4	9.49	1.64
69.2	9.54	1.29	70.1	9.52	1.60
69.1	9.53	1.50	70.1	9.49	1.49
69.1	9.54	1.37	70.2	9.51	1.41
73.3	9.50	1.69	73.9	9.51	1.44
73.3	9.50	1.38	74.0	9.50	1.45
73.4	9.51	1.49	73.9	9.49	1.42
77.7	9.50	1.47	78.0	9.46	1.44
78.0	9.51	1.41	78.1	9.46	1.35
78.0	9.51	1.37	77.9	9.44	1.36
81.2	9.50	1.39	81.8	9.45	1.48
81.2	9.49	1.31	81.7	9.45	1.46
80.9	9.49	1.41	81.7	9.45	1.46
85.0	9.46	1.44	85.8	9.43	1.55
84.9	9.46	1.36	85.8	9.43	1.33
84.9	9.46	1.45	85.8	9.46	1.42
89.0	9.46	1.37	89.2	9.45	1.47
89.1	9.46	1.27	89.1	9.45	1.47
89.3	9.46	1.32	89.0	9.45	1.32
92.4	9.45	1.38	92.7	9.45	1.39
92.3	9.45	1.36	92.8	9.46	1.45
92.1	9.46	1.26	92.8	9.44	1.35
96.1	9.46	1.28	96.1	9.45	1.30
96.2	9.46	1.36	96.2	9.45	1.35
96.4	9.46	1.19	96.2	9.44	1.27
99.7	9.45	1.29	99.5	9.45	1.31
99.7	9.45	1.15	99.4	9.45	1.23
99.3	9.45	1.32	99.5	9.47	1.11

Table 7. Measured damping of wing beam mode during Sweeps 2 and 6, the wing-off configuration

Straight Blades			Swept-Tip Blades		
Wind Speed (kt)	Frequency (Hz)	Damping (% critical)	Wind Speed (kt)	Frequency (Hz)	Damping (% critical)
30.4	5.05	0.48	30.3	5.07	0.42
30.3	5.05	0.53	30.5	5.07	0.46
30.5	5.05	0.52	30.3	5.07	0.52
40.3	5.04	0.51	40.3	5.07	0.54
40.4	5.04	0.45	40.4	5.07	0.41
40.4	5.04	0.49	40.4	5.06	0.38
50.4	5.04	0.67	50.7	5.07	0.52
50.6	5.04	0.73	50.5	5.07	0.88
50.3	5.04	0.62	50.5	5.07	0.62
60.3	5.04	0.71	60.2	5.07	0.57
60.5	5.02	0.91	60.4	5.07	0.61
60.1	5.04	0.71	60.6	5.06	0.68
65.4	5.04	0.79	65.2	4.99	0.94
65.4	5.04	0.66	65.1	4.98	0.82
65.2	5.04	0.62	65.1	4.98	0.64
70.4	5.05	0.83	70.1	5.01	0.56
70.4	5.05	0.72	70.1	4.98	0.69
70.5	5.05	0.97	70.1	4.99	0.81
74.4	5.03	0.79	74.4	4.98	0.47
74.5	5.04	0.89	74.3	4.98	0.69
74.9	5.04	0.83	74.5	5.01	0.62
79.2	5.06	0.90	78.6	4.97	0.99
79.2	5.06	0.66	78.5	5.01	1.34
79.1	5.04	0.81	78.4	5.00	1.09
82.9	5.04	0.79	82.0	5.00	0.82
82.8	5.04	0.80	82.2	4.98	1.06
83.0	5.06	0.83	82.3	4.98	0.84
86.3	5.06	1.17	86.1	4.99	1.10
86.7	5.06	0.61	86.1	5.01	1.06
86.6	5.06	0.94	86.1	5.02	1.59
89.8	5.05	1.26	89.7	5.05	0.85
89.8	5.03	1.03	89.6	5.04	0.99
89.9	5.06	1.04	89.5	5.04	1.01
93.7	5.04	0.53	93.1	5.05	1.02
93.9	5.04	0.62	93.4	5.04	0.93
93.8	5.04	0.94	93.4	5.05	0.85
97.5	5.06	0.91	97.0	5.05	0.99
97.6	5.05	0.88	96.8	5.04	1.14
97.4	5.06	1.36	96.6	5.04	0.77
100.8	5.09	1.01	100.0	5.04	0.94
100.8	5.08	0.76	100.1	5.05	0.60
100.8	5.06	0.89	100.2	5.07	1.54

Table 8. Measured damping of wing chord mode during Sweeps 2 and 6, the wing off configuration

Straight Blades			Swept-Tip Blades		
Wind Speed (kt)	Frequency (Hz)	Damping (% critical)	Wind Speed (kt)	Frequency (Hz)	Damping (% critical)
31.0	9.46	1.27	30.4	9.51	1.29
30.2	9.49	1.51	30.3	9.50	1.24
30.1	9.49	1.46	30.2	9.50	1.32
40.5	9.43	1.37	40.4	9.47	1.39
40.4	9.43	1.31	40.2	9.47	1.26
40.3	9.43	1.38	40.4	9.47	1.36
49.9	9.45	1.24	50.6	9.48	1.28
50.3	9.44	1.30	50.7	9.48	1.30
50.2	9.42	1.27	50.7	9.48	1.26
60.2	9.45	1.25	60.2	9.50	1.34
60.0	9.45	1.24	60.5	9.50	1.35
60.1	9.45	1.29	60.2	9.50	1.31
65.2	9.45	1.34	65.1	9.50	1.46
65.3	9.46	1.27	65.0	9.44	1.30
65.3	9.45	1.31	65.2	9.46	1.26
70.3	9.47	1.13	70.2	9.45	1.67
70.2	9.47	1.09	70.2	9.43	1.54
70.3	9.48	1.19	70.0	9.49	1.71
74.5	9.47	1.12	74.9	9.42	1.65
74.4	9.48	1.21	74.6	9.41	1.56
74.6	9.48	1.25	74.6	9.42	1.58
79.3	9.48	1.27	78.1	9.43	1.34
79.2	9.49	1.39	78.3	9.42	1.64
79.0	9.48	1.43	78.2	9.42	1.55
82.9	9.47	1.30	82.4	9.44	1.81
83.2	9.46	1.25	82.3	9.40	1.64
82.9	9.45	1.25	82.1	9.39	1.70
86.3	9.45	1.23	86.1	9.40	1.38
86.6	9.45	1.20	86.2	9.42	1.36
86.7	9.45	1.27	86.1	9.42	1.62
90.0	9.46	1.22	89.5	9.41	1.23
90.0	9.47	1.25	89.7	9.42	1.26
89.9	9.47	1.08	89.5	9.41	1.19
93.8	9.45	1.06	93.2	9.44	1.38
93.7	9.44	1.01	93.1	9.43	1.39
93.8	9.43	1.19	93.1	9.42	1.37
97.5	9.41	1.13	96.9	9.43	1.38
97.4	9.43	1.21	96.8	9.41	1.30
97.4	9.42	1.10	96.8	9.42	1.27
100.7	9.39	1.10	100.1	9.41	1.18
100.7	9.38	1.12	100.2	9.42	1.20
100.8	9.40	1.22	100.0	9.42	1.39

Table 9. Measured damping of wing beam mode during Sweeps 3 and 7, the gimbal locked configuration

Straight Blades			Swept-Tip Blades		
Wind Speed (kt)	Frequency (Hz)	Damping (% critical)	Wind Speed (kt)	Frequency (Hz)	Damping (% critical)
30.7	5.06	0.31	30.3	5.08	0.42
30.6	5.06	0.44	30.4	5.08	0.43
30.7	5.05	0.23	30.5	5.07	0.40
40.5	5.06	0.43	40.3	5.07	0.33
40.4	5.06	0.60	40.3	5.07	0.52
40.3	5.04	0.49	40.3	5.07	0.43
50.6	5.06	0.48	50.5	5.07	0.44
50.6	5.04	0.55	50.5	5.07	0.47
50.7	5.05	0.47	50.5	5.07	0.77
60.4	5.05	0.50	60.6	5.06	0.72
60.4	5.04	0.62	60.4	5.07	0.79
60.5	5.05	0.63	60.5	5.07	0.50
			66.9	5.07	0.83
			67.1	5.06	0.70
			67.2	5.06	0.80
			71.8	5.06	0.53
			72.1	5.07	0.70
			72.1	5.07	0.84
			76.4	5.07	0.80
			76.5	5.05	0.96
			76.5	5.07	0.74
			80.6	5.07	0.71
			80.8	5.05	0.70
			80.7	5.07	1.06
			84.9	5.06	0.89
			85.0	5.07	0.71
			84.8	5.06	0.55

Table 10. Measured damping of wing chord mode during Sweeps 3 and 7, the gimbal locked configuration

Straight Blades			Swept-Tip Blades		
Wind Speed (kt)	Frequency (Hz)	Damping (% critical)	Wind Speed (kt)	Frequency (Hz)	Damping (% critical)
30.4	9.50	2.13	30.4	9.45	2.33
30.0	9.48	2.07	30.3	9.46	2.31
30.7	9.50	2.13	30.5	9.43	2.32
40.4	9.49	1.93	40.4	9.41	2.20
40.3	9.48	1.91	40.4	9.41	2.24
40.4	9.49	2.07	40.4	9.40	2.18
50.6	9.46	1.86	50.6	9.39	2.29
50.6	9.46	2.02	50.5	9.42	2.33
50.6	9.46	1.84	50.4	9.40	2.26
60.5	9.44	1.68	60.5	9.39	2.13
60.6	9.45	1.76	60.5	9.39	2.14
60.5	9.45	1.77	60.5	9.39	2.15
			67.2	9.40	2.02
			67.0	9.39	2.36
			67.0	9.38	2.19
			71.7	9.38	2.02
			71.8	9.41	2.10
			71.8	9.42	2.09
			76.4	9.41	2.06
			76.5	9.37	2.09
			76.4	9.35	2.03
			80.6	9.37	2.08
			80.8	9.36	1.95
			80.8	9.34	2.15
			84.7	9.33	1.89
			84.7	9.36	2.04
			84.7	9.33	2.06

Table 11. Measured damping of wing beam mode during Sweeps 4 and 8, the powered configuration

Straight Blades			Swept-Tip Blades		
Wind Speed (kt)	Frequency (Hz)	Damping (% critical)	Wind Speed (kt)	Frequency (Hz)	Damping (% critical)
3.9	5.07	0.55	2.7	5.07	0.52
3.9	5.04	0.43	3.5	5.06	0.37
3.9	5.05	0.69	3.8	5.06	0.49
20.1	5.04	0.34	20.8	5.08	0.54
20.0	5.00	0.71	20.9	5.07	0.34
20.0	5.04	0.32	20.2	5.07	0.55
30.2	5.06	0.60	30.4	5.07	0.67
30.0	5.06	0.61	30.4	5.08	0.38
30.0	5.04	0.39	30.5	5.07	0.49
40.1	5.05	0.80	40.6	5.06	0.60
40.2	5.04	0.45	40.6	5.07	0.60
40.1	5.06	0.60	40.7	5.06	0.62
50.3	5.05	0.49	50.8	5.06	0.85
50.2	5.04	0.79	50.7	5.05	0.68
50.3	5.03	0.55	50.4	5.04	0.65
58.8	5.05	0.51	60.7	5.06	0.63
59.3	5.05	0.84	60.7	5.04	0.73
60.1	5.04	0.81	60.7	5.06	0.90

Table 12. Measured damping of wing chord mode during Sweeps 4 and 8, the powered configuration

Straight Blades			Swept-Tip Blades		
Wind Speed (kt)	Frequency (Hz)	Damping (% critical)	Wind Speed (kt)	Frequency (Hz)	Damping (% critical)
3.3	9.44	2.36	4.0	9.47	2.30
3.7	9.38	2.33	3.9	9.46	2.23
3.8	9.46	2.20	4.0	9.45	2.43
19.8	9.44	2.76	19.9	9.37	2.25
19.9	9.47	2.94	21.2	9.40	2.28
19.8	9.46	2.66	20.0	9.38	2.16
30.2	9.42	2.78	30.8	9.38	2.37
30.0	9.47	2.99	30.6	9.38	2.26
30.1	9.45	2.74	30.5	9.38	2.28
40.1	9.43	2.74	40.2	9.38	2.01
40.1	9.45	2.44	40.2	9.40	2.14
40.1	9.47	2.44	40.1	9.38	2.05
50.1	9.43	2.74	50.4	9.39	1.90
50.0	9.45	2.44	50.4	9.38	1.74
50.0	9.47	2.44	50.7	9.37	1.94
60.4	9.44	2.07	60.2	9.39	1.90
60.1	9.44	2.44	60.7	9.38	1.74
60.2	9.46	2.13	60.6	9.37	1.94

References

[1]Sutherland, J., Tsai, F., and Datta, A. "Whirl Flutter Test of the Maryland Tiltrotor Rig: Swept-Tip Blades," AIAA 2022-0568, Proceedings of the AIAA SciTech Forum, San Diego, CA, January 3–7, 2022.

[2]Datta, A., Tsai, F., and Sutherland-Foggio, J., "Design of A New Tiltrotor Test Facility at the University of Maryland," Proceedings of AIAA SciTech 2019 Forum, San Diego, CA, January 7–11, 2019.

[3]Tsai, F., Sutherland-Foggio, J., Datta, A., and Privett, D. "The Maryland Tiltrotor Rig (MTR): The Baseline Gimballed Hub," Proceedings of the 75th Annual Forum of the Vertical Flight Society, Philadelphia, PA, May 13–16, 2019.

[4]Sutherland, J., and Datta, A., "Fabrication, Testing, and 3-D Comprehensive Analysis of Swept Tip Tiltrotor Blades," *Journal of the American Helicopter Society*, **68**, 012002 (2023), DOI: 10:4050/JAHS.68.012002.

[5]Morin, A. "Fabrication, Wind Tunnel Testing, and Freewheeling Analysis of 4.75-ft Diameter Composite Tiltrotor Blades," M.S. Dissertation, University of Maryland, College Park, 2021.

[6]Tsai, F., Sutherland, J., Akinwale, A., Morin, A., Gul, S., and Datta, A., "Development and Whirl Flutter Test of the Maryland Tiltrotor Rig," *Journal of the American Helicopter Society*, submitted for publication.

[7]Gul, S., and Datta, A., "Prediction of Parametric Whirl Flutter Test Data," *Journal of the American Helicopter Society*, submitted for publication.

[8]Ham, N. D., Bauer, P. H., Lawrence, T. H., and Yasue, M., "A Study of Gust and Control Response of Model Rotor-Propellers in a Wind Tunnel Airstream," NASA CR 137756, 1975.

[9]Ham, N. D., and Whitaker, H. P., "A Wind-Tunnel Investigation of Tilt-Rotor Gust Alleviation System," NASA CR 152264, 1978.

[10]Popelka, D., Sheffler, M., and Bilger, J., "Correlation of Test and Analysis for the 1/5-Scale V-22 Aeroelastic Model," *Journal of the American Helicopter Society*, Vol. 32, (2), April 1987, pp. 23–33. DOI: 10:4050/JAHS.32.21.

[11]Piatak, D., Kvaternik, R. G., Nixon, M. W., Langston, C. W., Singleton, J. D., Bennett, R. L., and Brown, R. K., "A Parametric Investigation of Whirl-Flutter Stability on the WRATS Tiltrotor Model," *Journal of the American Helicopter Society*, Vol. 47, (2), April 2002, pp. 134–144. DOI: 10:4050/JAHS.47.134.

[12]Nixon, M. W., Langston, C. W., Singleton, J. D., Piatak, D. J., Kvaternik, R. G., Corso, L. M., and Brown, R. K., "Aeroelastic Stability of a Four-Bladed Semi-Articulated Soft-Inplane Tiltrotor Model," Proceedings of the International Forum on Aeroelasticity and Structural Dynamics, Amsterdam, the Netherlands, June 4–6, 2003.

[13]Kreshock, A. R., Thornburgh, R. P., and Wilbur, M. L., "Overview of the TiltRotor Aeroelastic Stability Testbed," AIAA 2022-0566, Proceedings of the AIAA SciTech Forum, San Diego, CA, January 3–7, 2022.

[14]Matuska, D., Dale, A., and Lorber, P., "Wind Tunnel Test of a Variable-Diameter Tiltrotor (VDTR) Model," NASA CR 177629, 1994.

[15]Johnson, J. L., and Young, L. A., "Tilt Rotor Aeroacoustic Model Project," Proceedings of the Confederation of European Aerospace Societies (CEAS) Forum on Aeroacoustics of Rotorcraft and Propellers, Rome, Italy, June 17–20, 1999.

[16]Srinivas, V., Chopra, I., and Nixon, M., "Aeroelastic Analysis of Advanced Geometry Tiltrotor Aircraft," *Journal of the American Helicopter Society,* Vol. 43, (3), July 1998, pp. 212–221, DOI: 10.4050/JAHS.43.212.

[17]Barkai, S. M., and Rand, O., "The Influence of Composite Induced Couplings on Tiltrotor Whirl Flutter Stability," *Journal of the American Helicopter Society*, Vol. 43, (2), April 1998, pp. 133–145, DOI: 10.4050/JAHS.43.133.

[18]Nixon, M. W., Piatak, D., Corso, L., and Popelka, D., "Aeroelastic Tailoring for Stability Augmentation and Performance Enhancements of Tiltrotor Aircraft," *Journal of the American Helicopter Society*, Vol. 45, (4), October 2000, pp. 270–279, DOI:10.4050/JAHS.45.270.

[19]Acree, C. W., "Effects of V-22 Blade Modifications on Whirl Flutter and Loads," *Journal of the American Helicopter Society*, Vol. 50, (3), July 2005, pp. 269–278, DOI: 10.4050/1.3092863.

[20]Bartie, K., Alexander, H., McVeigh, M., La Mon, S., and Bishop, H., "Hover Performance Tests of Baseline Metal and Advanced Technology

Blade (ATB) Rotor Systems for the XV-15 Tilt Rotor Aircraft," NASA CR 177436, 1988.

[21]Krüger, W. "Multibody Analysis of Whirl Flutter Stability on a Tiltrotor Wind Tunnel Model," *Proceedings of the Institution of Mechanical Engineers, Part K: Journal of Multi-Body Dynamics*, Vol 230, (2), May 2016, pp. 121-133, DOI: 10.1177/1464419315582128.

[22]Beaumier, P., Decours, J., and Lefebvre, T. "Aerodynamic and Aero-Acoustic Design of Modern Tilt-Rotors: The ONERA Experience," Proceedings of the 26th ICAS Congress, Anchorage, AK, September 14–19, 2008.

[23]Tsai, F. "Development of the Maryland Tiltrotor Rig (MTR) and Whirl Flutter Stability Testing," Ph.D. Dissertation, University of Maryland, College Park, 2022.

[24]Datta, A. "X3D - A 3-D Solid Finite Element Multibody Dynamic Analysis for Rotorcraft," Proceedings of the American Helicopter Society Technical Meeting on Aeromechanics Design for Vertical Lift, San Francisco, CA, January 20–22, 2016.

[25]Chi, C., Datta, A., Chopra, I., and Chen, R., "Three-Dimensional Strains on Twisted and Swept Composite Rotor Blades in Vacuum," *Journal of Aircraft*, Vol. 58, (1), 2021, pp. 1–16, DOI: 10.2514/1.C035746.